Annals of Biomedical Engineering, Vol. 16, pp. 349-365, 1988
Printed in the USA.

0090-6964/88 $3.00 + .00

MATHEMATICAL EVIDENCE FOR FLOW-INDUCED CHANGES IN MYOCARDIAL OXYGEN CONSUMPTION

Stan A. Napper, Roy W. Schubert

Department of Biomedical Engineering and
Center for Rehabilitation Science and Biomedical Engineering
Louisiana Tech University

(Received 5/29/87)

The objective of this investigation was to aid in the determination of the mechanism by which oxygen consumption changes in proportion to coronary perfusion pressure or coronary blood flow. A mathematical model of oxygen transport and consumption in the isolated-perfused heart was developed, based on data from an autoregulating, cell-free perfused, externally paced, isovolumic feline heart preparation. The model features the unique combination of Michaelis-Menten kinetics, and one-dimensional (axial) diffusion in radially well-mixed tissue. An adaptive finite-difference integration routine was used to solve the resulting third order stiff two-point boundary value problem. A simplex minimization was employed to determine the parameter values that minimized the squared difference between the model and the experimental data in terms of tissue PO_2 distribution (histograms). Different cases of the model representing pressure-induced, flow-induced, and "magnified" flow effects were run. The flow-dependent oxygen consumption version of the model produced a histogram squared error 30% lower than the pressure-induced version and 5% lower than any other case. The model and a critical review of the literature indicate that a flow-related mechanism is responsible for this phenomenon. Evidence also demonstrates that the Michaelis-Menten kinetics constant is not constant for different oxygen tensions.

Keywords—*Oxygen consumption, Heart, Model, Flow.*

INTRODUCTION

The relationship between coronary perfusion pressure and myocardial oxygen consumption was first described by Gregg (16). When coronary perfusion pressure or coronary blood flow increases, so does whole organ oxygen consumption (9,17,38). This observation was called Gregg's phenomenon (10). The mechanisms involved in

Acknowledgment—This work was published in fulfillment of the requirements for the Doctor of Philosophy in Biomedical Engineering at Louisiana Tech University in May, 1985. The authors express gratitude for technical advice offered by Dr. J.E. Fletcher of the Applied Mathematics Laboratory of NIH and financial support provided by NIH grant #HL22864 (RWS—Principal Investigator). James Cronk assisted through his parallel work in this laboratory with a linearized model.

Address correspondence to Stan Napper, Ph.D., Biomedical Engineering, P.O. Box 10348, Louisiana Tech University, Ruston, LA 71272.

this phenomenon have been a subject of some controversy. The focus of this controversy appears to be related to whether the phenomenon is pressure-induced or flow-induced (2,3).

The pressure-induced oxygen consumption hypothesis proposes that the increased pressure in the vessels alters the length of the myocardial fibers, similar to the effect of increased pressure in a garden hose, invoking the Frank-Starling law of the heart (18,27). A variety of experiments and experimental conditions have led researchers to decide in favor of this hypothesis (2,3,25,35) or similar pressure-related mechanisms (30,43).

The flow-induced hypothesis is described as better perfusion of previously underperfused areas. According to this theory, since the heart operates normally at low PO_2 (40,41), when flow is increased more of the tissue is better supplied with oxygen (1,4,5,9,11,44). A flow-induced mechanism may also be explained by washout of metabolites (1,28,44) or a decrease in local hypoxia near single capillaries (32). Scharf and Bromberger-Barnea (36) concluded that the phenomenon is due to capillary hydrostatic pressure which is complexly related to flow, perfusion pressure, and venous pressure.

Mathematical models had not been specifically applied to the evaluation of the proposed mechanisms of Gregg's phenomenon. A model capable of reflecting and comparing both a pressure-induced mechanism and a flow-induced mechanism and based at the capillary-tissue level oxygen transport should clarify this controversy. Use of Michaelis-Menten kinetics for the oxygen consumption rate provides this capability. A linearized approximation to Michaelis-Menten kinetics (8) suggested the importance of developing the complete nonlinear model. Therefore, we have derived a mathematical model that includes both mechanisms and have matched the model results with reported isolated heart data (36,37).

METHODS

Mathematical Model

Mathematical models of physiological transport processes can be extremely useful because the microscopic level at which many of these processes occur resists direct measurement. The mathematical model can incorporate indirect or boundary measurements and whole-organ parameter values to produce a more complete picture of capillary-tissue exchange (12). Mathematical models of oxygen transport date back to 1918 (20) and the work of A. Krogh, in which the supply and demand of oxygen are modeled as a cylindrical capillary which supplies oxygen to a concentric annulus of tissue consuming oxygen at a constant rate (Fig. 1). The modeling literature has been reviewed elsewhere (12,19,22).

The derivation of the basic model upon which the presented model is built has been published elsewhere (39). The modeling assumptions used in this investigation include (26):

1. Radially well-mixed tissue;
2. Michaelis-Menten kinetic oxygen consumption;
3. Homogeneously distributed oxygen consumption kinetics;
4. Straight, parallel, concurrent, homogeneously distributed capillaries;
5. Space-averaged capillary wall permeability based on radially well-mixed tissue;

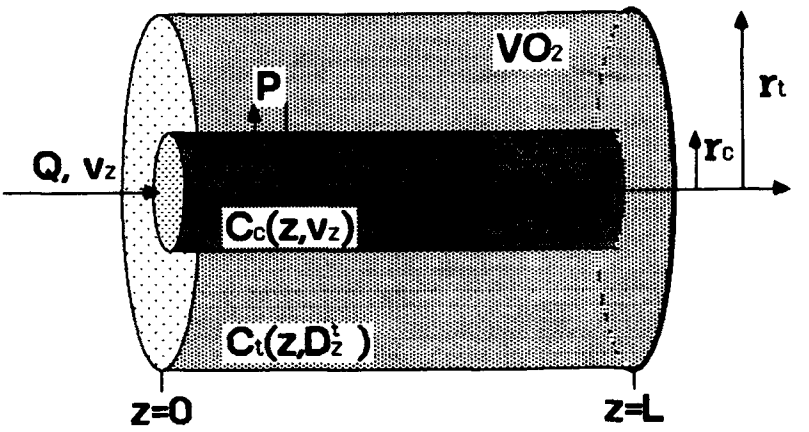

FIGURE 1. Krogh capillary-tissue cylinder.

6. Isotropic diffusion;
7. Steady state;
8. No-flux boundary conditions.

These assumptions produce the following equations:

$$\text{Capillary:} \quad \frac{dC_c}{dz} = \frac{2P(C_t - C_c)}{v_z r_c} \tag{1}$$

$$\text{Tissue:} \quad \frac{d^2C_t}{dz^2} = \frac{2Pr_c(C_t - C_c)}{D_z^t(r_t^2 - r_c^2)} + \frac{V_{\max}C_t}{D_z^t S_o^t(C_t + K_m)} \tag{2}$$

$$\text{Boundary Conditions:} \quad C_c(0) = C_{cA} \tag{3}$$

$$\frac{dC_t(0)}{dz} = 0 \tag{4}$$

$$\frac{dC_t(L)}{dz} = 0 \tag{5}$$

Equation 1 is the first order differential equation relating the axial change in capillary oxygen tension to capillary wall permeability, P, and the radial oxygen concentration gradient, where C is oxygen tension (in tissue, t, and capillary, c), z is the axial dimension, r_c is the radius of the capillary, and v_z is the capillary linear velocity. Equation 2 is the second order differential equation relating axial tissue O_2 change to the radial flux across the capillary wall into the tissue and the tissue oxygen consumption. $V_{\max}$ is maximum oxygen consumption, Km is the Michaelis-Menten kinetics constant, D_z^t is the axial tissue diffusion coefficient, r_t is the tissue radius, and S_o^t is the tissue oxygen solubility relating concentration to partial pressure.

Description of Experiment Modeled

The experiment from which the data were taken (40) is well suited for a synergistic mathematical investigation because of the conditions of the heart; namely, isolated, autoregulating, isovolumic, hemoglobinless, cell-free perfused heart. This experiment reduces the number of independent variables that could affect the oxygen consumption by: (a) pacing (eliminating time-dependent phenomena), (b) isolating the organ from systemic nervous intervention, (c) providing a constant volume for the heart muscle to contract against, and (d) eliminating nonlinear capillary transport processes. The normal response to a 40% increase in perfusion pressure was a slight (less than 10%) though significant increase in flow, ventricular function, and oxygen consumption, indicating good regulation of these variables (40). The Whalen-type oxygen microelectrode (45) was used to obtain oxygen tension histograms (Figs. 2a and 2b). The sampling was done so that the histogram could be viewed as a probability density function. The major conclusions of this experiment were that locally hypoxic areas of the tissue make up a significant tissue volume (10–15%), that these areas may serve as a feedback signal for microvascular adjustment and that a common control mechanism may be operating to achieve oxygen mass balance in response to both perfusion pressure changes and altered oxygen supply and demand (40).

Other features of the presented model include the use of whole organ experimentally measured constraints. The following set of equations were used to constrain the model to correspond to the experiment (as in ref. 8):

$$v_z = \frac{QL}{N\pi r_c^2} \tag{6}$$

$$r_t^2 = \frac{(1 + N\pi r_c^2)}{N} \tag{7}$$

Equation 6 relates the capillary fluid velocity, v_z, to the whole organ flow, Q (an experimentally measured parameter), the capillary length, L, and the capillary cross-sectional area, r_c^2, through the capillary density, N. The second constraint (Eq. 7) relates the tissue annulus radius to the capillary density under the assumption that a series of parallel, cylindrical capillaries completely covers the metabolizing tissue cross section (8,37). Since the value for oxygen extraction, E, was known from the experiment (40), it was used as an additional constraint in that the computed extraction for the model was forced to be the same.

Mathematical Protocol

The model was used to evaluate the two hypotheses which have been considered as explanations for Gregg's phenomenon as described above (pressure-induced or flow-induced). Use of a Michaelis-Menten kinetics rate expression in this axially distributed model provides three possible methods for modulation of oxygen consumption: (a) PO_2 increases, (b) Km decreases, or (c) V_{max} increases. A pressure-induced (garden hose) modulation would affect oxygen consumption throughout the tissue (along the total tissue cylinder length), even at high PO_2 values. Therefore, a pressure-induced response can be modeled as changes in V_{max}. A flow-induced mecha-

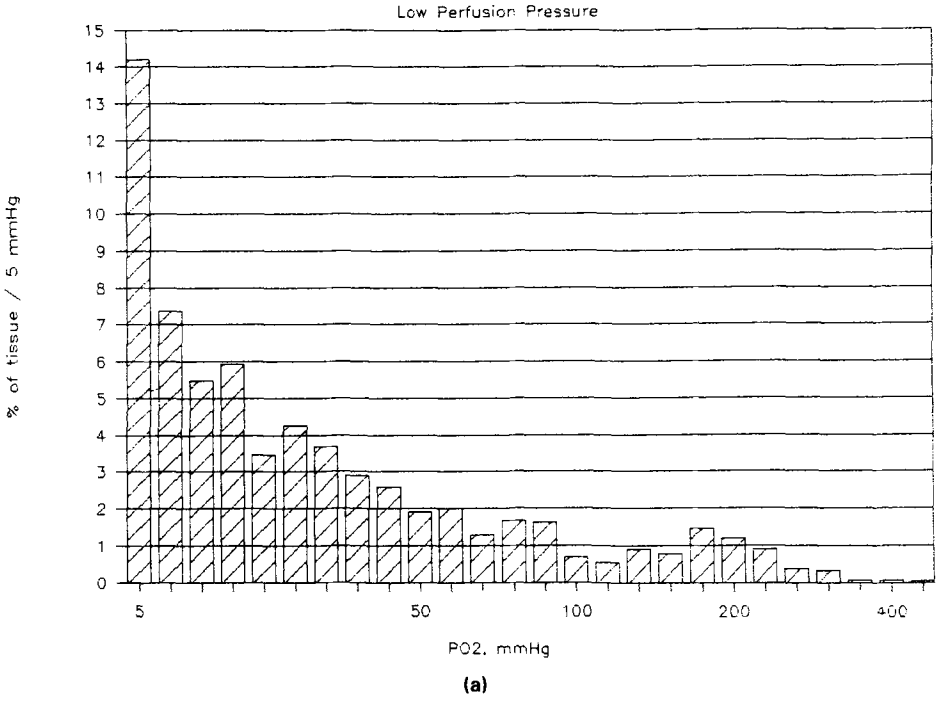

(a)

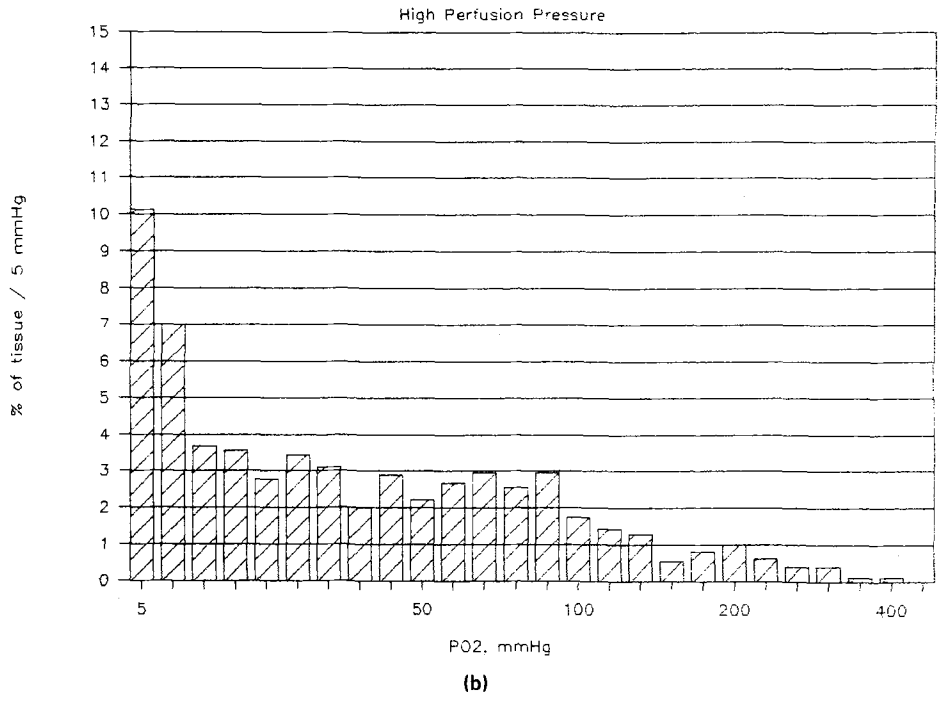

(b)

FIGURE 2. Experimental PO_2 histograms; (a) Low perfusion pressure, (b) High perfusion pressure.

nism, better perfusion of previously underperfused areas, results in increased tissue oxygen tension (concentration) and a rightward shift in the PO_2 histogram. Table 1 summarizes the protocol for the modeling experiment in relation to the different mechanisms under investigation. Different cases of the model correspond to different theories. In Case 1, where *Km* is 0, the simplex routine was used to find the values of D_z^t which minimize the error criterion. In this case, modulation of oxygen consumption is achieved strictly through changes in the whole organ consumption rate (VO_2). Here it is assumed that changes in VO_2 are related to the change in perfusion pressure by some mechanism like the hydrostatic capillary pressure (36), where VO_2 is the zero-order consumption rate calculated from the experimentally measured extraction and flow (38,40). Modulation of oxygen consumption strictly by flow (or supply) is modeled in Case 2 by Michaelis-Menten kinetics. The simplex routine finds the optimal values of *Km*, V_{max}, and D_z^t. A possible combined effect of flow- and pressure-induced mechanisms may be modeled (as in Case 3) by allowing V_{max} to vary from low to high perfusion pressure with fixed *Km*. In Case 4, variable *Km* "magnifies" the flow dependence of VO_2 as V_{max} is fixed from low to high perfusion pressure. Finally, the combined effect of flow, pressure, and a "magnified" flow effect is studied by allowing both *Km* and V_{max} to change with perfusion pressure.

Numerical Considerations

The model equations form a stiff, two-point boundary value problem (15). The solution technique employed is a variable order, variable step, finite difference routine for nonlinear systems with two-point boundary conditions called PASVA (21). PASVA has been demonstrated to be very successful with stiff boundary value problems (14). This numerical technique permitted solution of the linear case of the model (39) to within 10^{-5} of the analytically computed solution for any given axial distance. Subsequent computations were performed with a relative error tolerance of 10^{-8} to ensure accurate solutions for the nonlinear equations. The additional accuracy was imposed at a relatively minor cost (about 1 second of computer processor time per solution).

The experimental data used as modeling constraints, or as data to be matched, are frequency distributions of the tissue volume per 5 mmHg increment of measured PO_2 (Figs 2a and 2b, from 40). Computed tissue volume histograms are compared

TABLE 1. Mathematical protocol (model descriptions).

Case	*Km*	V_{max}	Description
1.	0	VO_2	Basic model, pressure-induced VO_2 modulation
2.	*F*	*F*	Flow-induced VO_2 modulation
3.	*F*	*V*	Pressure and flow both modulating VO_2
4.	*V*	*F*	"Magnified" flow-induced VO_2 modulation
5.	*V*	*V*	Pressure and "magnified" flow-induced VO_2 modulation

F = fixed from low perfusion pressure to high perfusion pressure (LO value = HI value).
V = variable from low perfusion pressure to high perfusion pressure (LO value ≠ HI value).

to experimental histograms. The most widely used criterion for selecting the best model is the minimization of the sum of squared error (14). The histogram squared error for each of two perfusion pressures ("high" and "low") is the sum of the squared differences between computed and actual frequency values. Each squared difference is weighted by the variance observed in the measurements and by the total number of observations (37). This error is minimized by the modified sequential simplex method (29). For this model with less than 10 variables to be simplexed and for a very sensitive system of equations, this slowly converging, nongradient simplex method is appropriate. Since the histograms for the two perfusion pressures were of equal importance, the two squared errors were also forced to be equal. In other words, the model was constrained to match the low pressure data equally as well as the high pressure data. This constraint has not been documented before, even in the related work with the linearized model (8). This requirement was implemented by adding the squared difference between the two histogram squared errors to the simplex minimization function. The final function which the simplex routine sought to minimize was the sum of the histogram squared errors, the squared difference between model and experimental extraction rates, and the squared difference between total low pressure histogram squared error and total high pressure histogram squared error.

Table 2 gives the values of parameters of the model for low and high perfusion pressures. Perfusion pressure (PP) and Extraction (E) are experimental values given by Fletcher and Schubert (13) from the original experiments. The standard error of the mean (along with the number of data points) is given for the extraction rate because the extraction constraint on the model is considered to be met when the computed arteriovenous difference is in this interval. The flow rate, Q, is derived from the measured flow rate (40) and adjusted for left heart (84.4% of total weight), for the 0.15 ml blood volume per ml of vascular blood volume, and for the 80% moisture content. The whole organ consumption rate, VO_2, is calculated from the extraction and the flow using the solubility. The solubility of oxygen in tissue, S_o', is 0.025 ml O_2/ml tissue when the PO_2 is 760 mmHg, corrected for the temperature of the experiment (32.5°C). Capillary density (N), tissue radial diffusion coefficient (D_r'), capillary radius (r_c), and cylinder length (L) are typical values (6,7,13,33). Figures 2a and 2b show the experimental PO_2 histograms for low and high perfu-

TABLE 2. Parameter values for low (LO) and high (HI) perfusion pressures (PP).

	LO	HI	Units
PP	79.2	111.1	mmHg
E	620 ± 4	602 ± 5	mmHg
	(n = 98)	(n=98)	
Q	4.0303317	4.38595	ml/min-ml(tissue)
VO_2	3.27710×10^{-6}	3.46272×10^{-6}	molesO_2/min-ml
S_o'	1.31147×10^{-9}		molesO_2/mmHg-ml
N	300,000	200,000	capillaries/cm^2
D_r'	0.99×10^{-3}		cm^2/min
r_c	2.5×10^{-4}		cm
L	0.05		cm

sion pressures, respectively, measured and reported by Schubert (40) and used as the objective criterion for evaluating each case.

RESULTS

Table 3 presents the results of the simplex minimization for all five cases. Values are given for Km(LO), Km(HI), V_{max}(LO), V_{max}(HI), D_z^t/D_r^t, C_{cA}(LO), and C_{cA}(HI) which best match both the experimental histograms and the extraction constraints. The axial tissue diffusion coefficient is the only one of these optimized parameters which is never considered to change with the perfusion pressure. Table 4 presents the computed extractions for low and high (LO and HI) perfusion pressure data and also gives the histogram squared error (HERR) for each of the five cases. The simplex was restarted several times with different initial parameter values to rule out local minima (42). The reported values then are the coordinates of the simplex which produced the global minimum squared histogram error (HERR) and which conformed to the constraints imposed by the experiment.

Oxygen consumption profiles (VO_2 vs. z) have been computed for each of the five cases. Figures 3a–e indicate the effect that each set of modeling assumptions has on the oxygen consumption throughout the tissue cylinder, at least in the axial direction. These consumption profiles are calculated from the Michaelis-Menten kinetic

TABLE 3. Simplex parameter optimization results—five cases.

	Case Number				
	1	2	3	4	5
Km(LO) (mmHg)	0	3.98	4.24	4.54	4.99
Km(HI) (mmHg)	0	3.98	4.24	3.87	3.97
V_{max}(LO) $\times 10^6$ (molesO_2)/ml-min	3.28	3.97	3.94	4.02	4.05
V_{max}(HI) $\times 10^6$ (molesO_2)/ml-min	3.46	3.97	4.08	4.02	4.03
D_z^t/D_r^t	12.8	8.03	8.07	8.36	8.03
C_{cA}(LO) (mmHg)	620.1	623.8	619.4	621.1	621.9
C_{cA}(HI) (mmHg)	603.2	600.0	605.4	602.5	602.5

TABLE 4. Histogram Squared Error (HERR) and extraction results for five cases.

	Case Number				
	1	2	3	4	5
HERR $\times 10^{-4}$	2.43	1.99	1.78	1.76	1.71
E(LO) (mmHg)	620	622.2	617.5	619.3	617
E(HI) (mmHg)	602	597.7	602.6	599.8	602.7
C_{cA}(LO) (mmHg)	620	623.8	619.4	621.1	619
C_{cA}(HI) (mmHg)	603	600.9	605.4	602.5	605.7
C_{cV}(LO) (mmHg)	0.15	1.6	1.9	1.8	2.0
C_{cV}(HI) (mmHg)	1.16	3.2	2.7	2.7	3.0

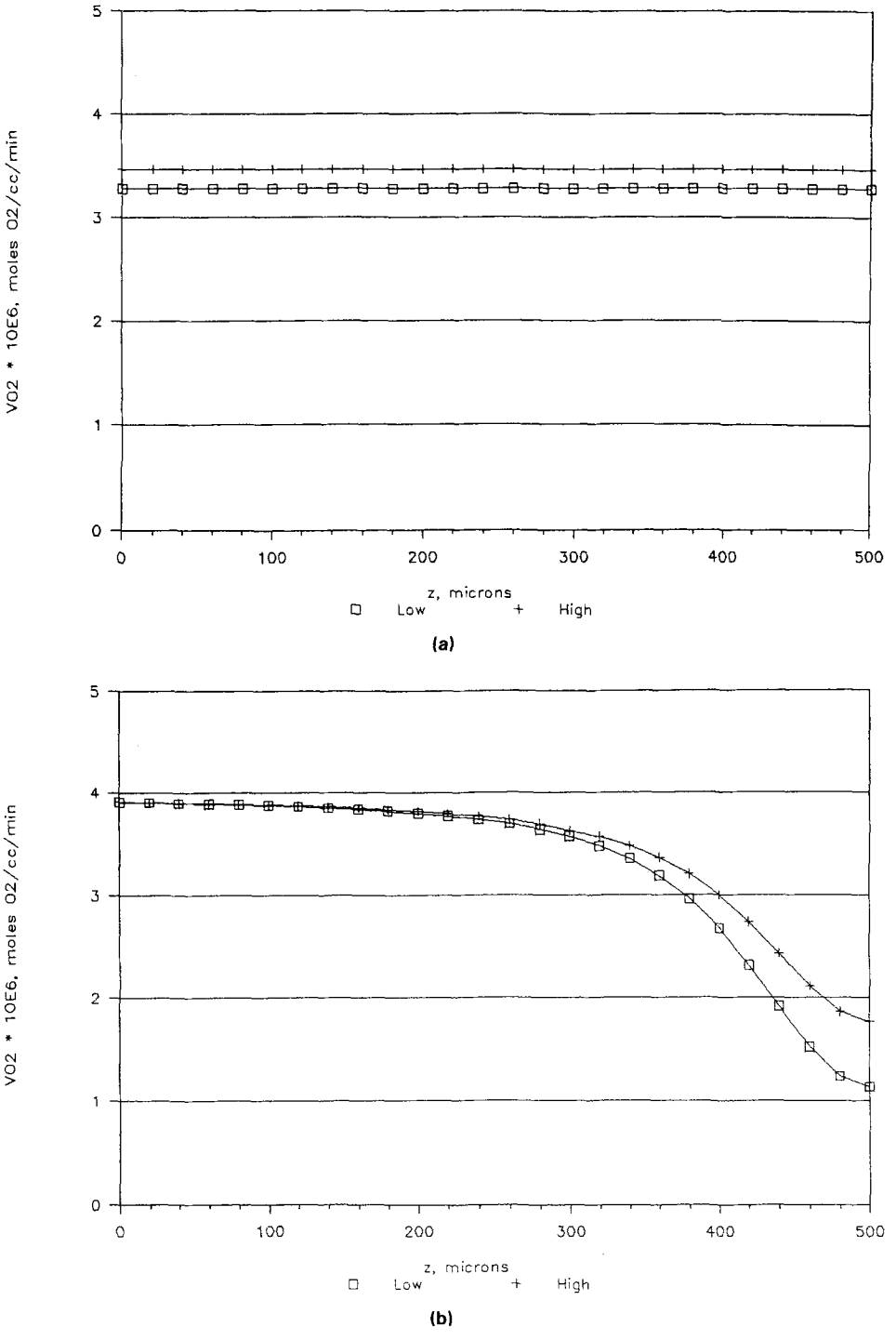

FIGURE 3. Oxygen consumption profiles for each of the five model cases.

Figure 3 continued on the following pages

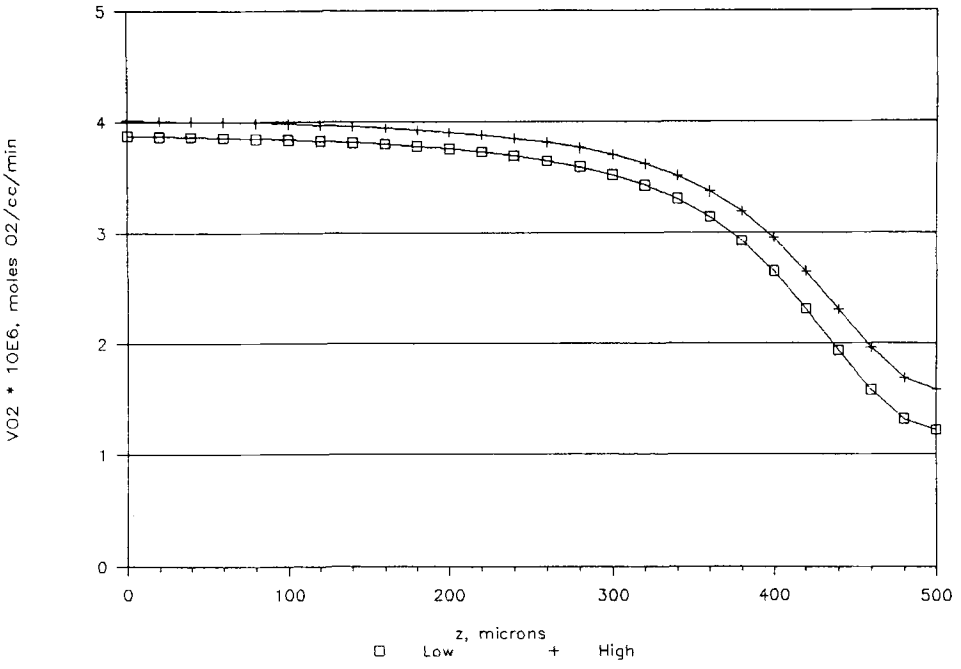

(c)

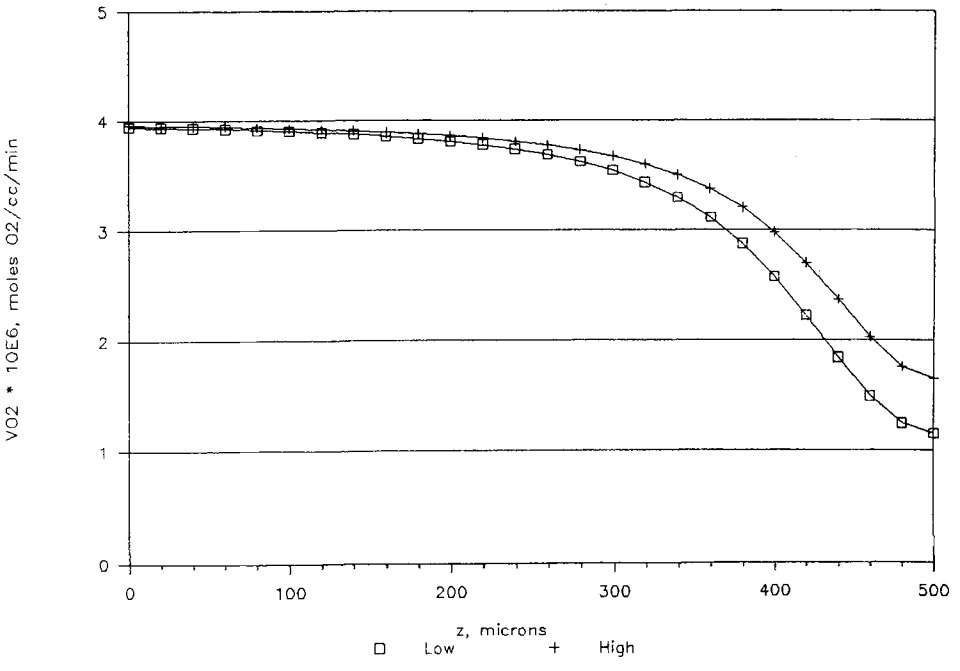

(d)

FIGURE 3 continued.

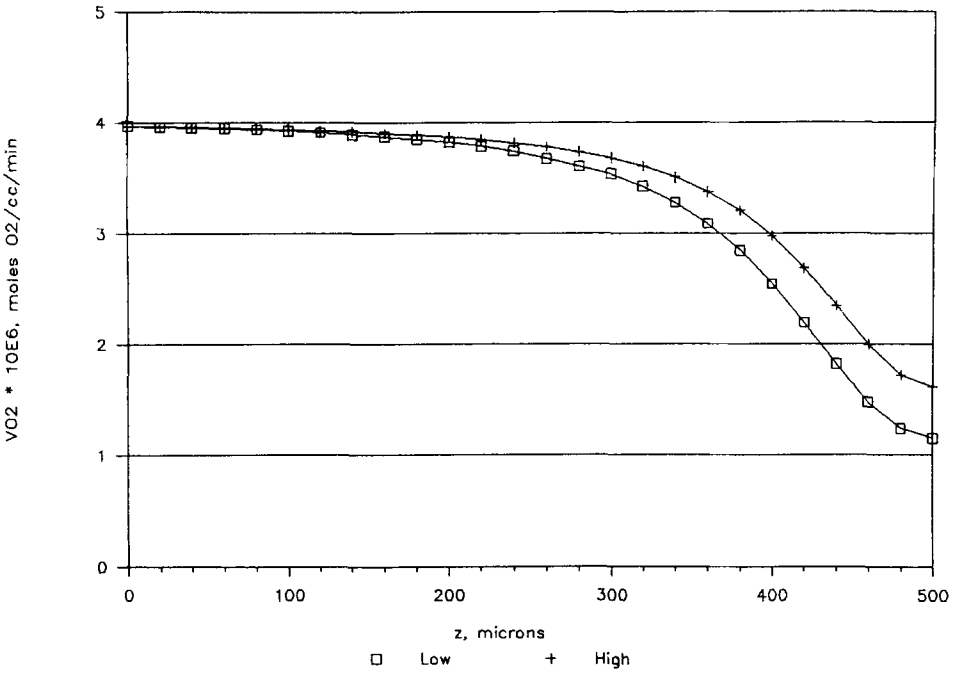

(e)

FIGURE 3 continued.

expression using the PO_2 values obtained from the numerical solution of the model equations.

(Case 1) Pressure Related:

In Fig. 3a, the oxygen consumption rate increased only with perfusion pressure. It is not clear whether this modulation in heart tissue occurs by means of a pressure-induced mechanism or a flow-induced mechanism.

(Case 2) Flow Related:

Figure 3b indicates the results of a flow-only mechanism for modulation of oxygen consumption in which the local consumption rate decreases for low values of PO_2 via Michaelis-Menten kinetics. This modulates whole organ oxygen consumption because the oxygen delivery is a function of flow. In essence, as perfusion pressure increased 40%, flow increased 10% during autoregulation (38,40) and the PO_2 histogram shifted rightward (higher percentage of higher PO_2 values). Therefore, the oxygen consumption was larger and the total histogram squared error was 7.5% less than in Case 1.

(Case 3) Combined Pressure and Flow:

Figure 3c presents the VO_2 profile for the combined mechanisms for consumption modulation in which the maximal consumption rate (V_{max}) is related to the pressure and Michaelis-Menten kinetics modulation produces flow dependent phenomena. The total histogram squared error was reduced by 26% over Case 1 by this assumption.

(Case 4) Variable Km:

Figure 3d shows the VO_2 profile computed for Case 4 in which V_{max} does not change with perfusion pressure, but *Km* is allowed to change. This results in a histogram error which is 30% lower than the Case 1 error and 5% lower than the Case 3 error.

(Case 5) Total Effect:

The VO_2 profile computed for Case 5 is shown in Fig. 3e. In this case, modulation of oxygen consumption by capillary perfusion pressure is permitted by allowing V_{max} to vary with perfusion pressure. Flow-dependent modulation is modeled again by Michaelis-Menten kinetics. The total computed histogram squared error was within 3% of the error of Case 4.

DISCUSSION

Radially Well-Mixing

The radially well-mixed model is based on the anatomical fact that capillaries in the heart are long and narrow (6,33). The length to diameter ratio is over 100 to 1 (33). In this model, radial transport from capillary to tissue is modeled by a finite capillary wall permeability, which is calculated from a space-average of the Krogh radial solution (i.e., the radial fluxes between the model and the Krogh radial solution are equal). The correct analytical solution of a two-dimensional model in which diffusion of oxygen was modeled in both the radial and axial directions and consumption was constant was developed (13). This solution has been used to quantify the true effects of axial diffusion in the heart (13). The assumption of radial well-mixing appears to be justified for the dimensions of capillaries in the heart (39).

Flow-Induced Mechanism

The minimum squared error over all cases was produced by Case 4 which modeled a flow-induced response (Michaelis-Menten kinetics) which is magnified at low PO_2 values (through changes in *Km*). Case 5 presented the optimization routine with the greatest degree of freedom in that all consumption parameters were free to change. However, the predicted V_{max} did not change significantly. If a pressure-related mechanism were chiefly involved, V_{max} should have increased in Case 5. Although the model indicates that a flow-related mechanism is the main cause of the oxygen consumption modulation, pressure-related mechanisms may not be completely ruled out. This is shown by a significant reduction in total histogram squared error in Case 3, compared with Case 1. In Case 3, oxygen consumption was modulated by a change in V_{max}. If the investigation had been stopped at this point, without con-

sidering variable *Km*, Case 3 would have indicated that Gregg's phenomenon is due to flow and pressure combined. However, a flow-induced mechanism, in which Michaelis-Menten kinetics with variable *Km* accounts for oxygen consumption modulation, appears to be the most likely explanation for Gregg's phenomenon. This conclusion is supported by recent single capillary measurements of oxygen transport which found a flow dependence of oxygen consumption in nearby tissues (32).

Critical Review of Literature on Gregg's Phenomenon

The conclusion favoring a flow-induced mechanism leads to further consideration of the literature reporting conclusions which support the alternate hypothesis. Criticisms of experiments which support a pressure-induced mechanism for Gregg's phenomenon fall into five categories: (a) nonworking preparations, (b) nonautoregulating preparations, (c) nonisovolumic preparations, (d) edematous preparations, and (e) inaccurate conclusions about the adequacy of oxygen supply based only on venous PO_2 determinations.

(a) Nonworking Hearts. Nonworking hearts (30) eliminate the metabolic influence of flow on heart function and may then miss the importance of coronary blood flow as a mediator of myocardial oxygen consumption. The experiment modeled here was a working (paced, constant load) isolated heart preparation (40).

(b) Nonautoregulating Hearts. Weisfeldt and Shock (44), in isovolumic hearts, pointed out the influence of autoregulation on the magnitude of the change in myocardial oxygen consumption as observed by Bacaner *et al.* (4). Schubert *et al.* (40), in isolated hearts displaying good autoregulation, found that the ability to autoregulate correlated with the ability to respond to induced changes in VO_2 and suggested that autoregulation keeps capillary pressure constant. This reflects negatively on experiments in which nonautoregulating hearts were used to determine the importance of coronary perfusion pressure (2,27).

(c) Nonisovolumic Preparations. Nonisovolumic preparations may show that changes in fiber length occur, which authors have sometimes attributed to the garden hose effect (1,27). This may, however, be attributable to increased load and the Frank-Starling mechanism rather than an increase in work due to the "stiffer" coronary vessels. The experiment modeled in this paper used isovolumic hearts so that length-dependent determinants of contractile strength were disregarded.

(d) Edematous Preparations. Weisfeldt and Shock (44) found that dextran was required in Krebs-Heinsleit perfused, isolated heart preparations to prevent edema by providing proper osmotic pressure. They criticized the work of Arnold *et al.* (2) because constant flow at higher pressures was maintained by the addition of dextran. However, no dextran was added to the control flow and pressure conditions so that an edematous preparation had unexpectedly developed. Morgenstern *et al.* (25) interpreted changes in myocardial wall thickness in terms of increased intracoronary blood volume whereas the edema in the preparation was not considered. Their measurement of blood volume was correlated with changes in myocardial fiber length, although this may be related to changes due to the Frank-Starling mechanisms as discussed above. Templeton *et al.* (43) found no changes in myocardial stiffness resulting from increased coronary perfusion pressure. They criticized the earlier work of Salisbury

et al. (34), who proposed an "erectile" effect of the coronary vasculature, based on the likelihood of edema formation.

(e) Adequate Oxygenation. Some authors have concluded against oxygen supply as the mediating factor of oxygen consumption on the basis of high recorded effluent oxygen tensions (27,31). However, the significance of low tissue PO_2 values, in spite of high venous values (10,40,45) has been missed or misunderstood. If some local areas of the tissue are hypoxic, as experimental PO_2 distributions indicate (see Figs. 2a and 2b), then the oxygen supply as determined by flow may be very significant for modulation of whole organ oxygen consumption.

(f) Conclusion. This review of conclusions which support the theory of a pressure-induced mechanism for Gregg's phenomenon provides further support for our conclusion that a flow-induced mechanism is responsible.

Variable Km

Since Michaelis-Menten kinetics is a chemical concept of enzyme rates, a biochemical explanation is sought to explain the significance of a variable *Km* as indicated by the model. Biochemical enzymatic kinetic theory describes two extremes for inhibition of enzyme regulated reactions (23,24). During competitive inhibition, the value of V_{max} does not change but *Km* does. The effect of a noncompetitive inhibitor is to decrease V_{max} without affecting *Km*. The model predicts that *Km* decreases while V_{max} remains relatively constant when flow increases. If these results can be interpreted in terms of competitive or noncompetitive inhibition, it appears that a competitive inhibition is occurring. This is because *Km* decreases roughly 20% as perfusion pressure increases, while V_{max} is statistically unchanged. The "true" value of *Km* is difficult to determine and a variety of values have been reported (26). The possibility of a variable *Km* is significant though only briefly considered in the literature (46).

Axial Diffusion Coefficient

Another result, which concerns the axial diffusion coefficient, supports the conclusion in favor of a flow-related mechanism. The value for tissue axial diffusivity in the linear, zero-order case was over 12 times the reported value, consistent with a previous finding of an elevated "effective" axial diffusion coefficient (40). The current model indicates that the need for a higher "effective" diffusion coefficient may be explained partially by decreased oxygen demand in areas which have low oxygen tension. The consumption rates are lower in these areas due to the Michaelis-Menten kinetics. However, zero-order consumption implies that the rate is constant even in the locally hypoxic areas. If this form of kinetics is applied physiologically, the oxygen transport would have to be greater to hypoxic areas in order to keep the tissue there viable. Thus, the diffusion coefficient was found to be higher when forced to match experimental data. A new estimate of diffusivity is eight times normal based on this mathematical model. This is taken as indirect support for a flow-induced mechanism because Michaelis-Menten kinetics modulates consumption as a result of oxygen supply and supply is related to flow, not pressure.

CONCLUSIONS

Two significant conclusions were indicated by the model. The first is that a flow-induced mechanism is primarily responsible for Gregg's phenomenon, rather than a pressure-induced mechanism. This is based on the histogram squared error results, the oxygen consumption profiles, a critical review of literature supporting a pressure-induced theory, and the reduced "effective" axial diffusion coefficient. The second important conclusion is that *Km* is variable as indicated by Case 4 of the model.

REFERENCES

1. Abel, R.M.; Reis, R.L. Effects of coronary blood flow and perfusion pressure on left ventricular contractility in dogs. Circ. Res. 28:961-971; 1970.
2. Arnold, G.; Kosche, F.; Miessner, E.; Neitzert, A.; Lochner, W. The importance of the perfusion pressure in the coronary arteries for the contractility and the oxygen consumption of the heart. Pflugers Archiv. 299:339-356; 1968.
3. Arnold, G.; Morgenstern, C.; Lochner, W. The autoregulation of the heart work by the coronary perfusion pressure. Pflugers Archiv. 321:34-55; 1970.
4. Bacaner, M.B.; Lioy, F.; Visscher, M. Induced change in heart metabolism as a primary determinant of heart performance. Am. J. Physiol. 209(3):519-531; 1965.
5. Bacaner, M.B.; Lioy, F.; Visscher, M. Coronary blood flow, oxygen delivery rate and cardiac performance. J. Physiol. 216:111-127; 1971.
6. Bassingthwaighte, J.B.; Yipintsoi, T.; Harvey, R.B. Microvasculature of the dog left ventricular myocardium. Microvasc. Res. 7:229, 1974.
7. Berne, R.M.; Rubio, R. Coronary circulation. In: Berne, R.M.; Sperelakis, N. eds. Handbook of Physiology: The Cardiovascular System. Washington D.C.: Am. Physiol. Soc., sect. 2, vol. I, Chapt. 25, 1980: pp. 873-952.
8. Cronk, J.W.; Schubert, R.W. Michaelis-Menten-like kinetics in the Krogh tissue cylinder. In: Bruley, D.F.; Bicher, H.I.; Reneau, D.D., eds. Oxygen transport to tissue—VI. New York: Plenum Press; 1985: pp. 499-510.
9. Daniell, H.B. Coronary flow alterations on myocardial contractility, oxygen extraction, and oxygen consumption. Am. J. Physiol. 225(5):1020-1025; 1973.
10. Feigl, E.O. Coronary physiology. Physiol. Rev. 63(1):1-205; 1983.
11. Fisher, V.J.; Martino, R.A.; Harris, R.S.; Kavaler, F. Coronary flow as an independent determinant of myocardial contractile force. Am. J. Physiol. 217(4):1127-1133; 1969.
12. Fletcher, J.E. Mathematical modeling of the microcirculation. Math. Biosci. 38:159-202; 1978.
13. Fletcher, J.E.; Schubert, R.W. Diffusional coupling in perfused capillary-tissue structures. In: Lübbers, D.W.; Acker, H.; Leniger-Follert, E., eds. Oxygen transport to tissue—VI. New York: Plenum Press; 1983.
14. Garfinkel, D.; Fegley, K.A. Fitting physiological models to data. Am. J. Physiol. 246:R641-650; 1984.
15. Gladwell, I. A survey of subroutines for solving boundary value problems in ordinary differential equations. In: Gladwell, Sayers, eds. Computational techniques for ordinary differential equations. New York: Academic Press; 1980: pp. 273-303.
16. Gregg, D.E. Regulation of the collateral and coronary circulation of the heart. Circulation. Oxford: Blackwell Scientific Publications; 1958.
17. Gregg, D.E. Effect of coronary perfusion pressure or coronary flow on oxygen usage of the myocardium. Circ. Res. 13:497-500; 1963.
18. Kahler, R.L.; Braunwald, E.; Kelminson, L.L.; Kedes, L.; Chidsey, C.A.; Segel, S. Effect of alterations of coronary blood flow on the oxygen consumption of nonworking heart. Circ. Res. 13:501-509; 1963.
19. Kreuzer, F. Oxygen supply to tissues: The Krogh unit and its assumptions. Experientia. 38:1415-1426; 1982.
20. Krogh, A. The rate of diffusion of gases through animal tissues with some remarks on the coefficient of invasion. J. Physiol. (London). 52:391; 1918.
21. Lentini, M.; Peyrera, V. An adaptive finite difference solver for nonlinear two-point boundary problems with mild boundary layers. SIAM J. Num. Anal. 14:91-111; 1979.

22. Leonard, E.F.; Jorgensen, S.B. The analysis of convection and diffusion in capillary beds. Ann. Rev. Biophys. Bioeng. 3:293-339; 1974.
23. Mattiazzi, A.R.; Congolani, H.E.; deCastumam, E.S. Relationship between calcium and hydrogen ions in heart muscle. Am. J. Physiol. 237(4):H497-H503; 1979.
24. McGilvrey, R.W. Biochemistry. Philadelphia: W.B. Saunders Co; 1970.
25. Morgenstern, C.; Holjes, U.; Arnold, G.; Lochner, W. The influence of coronary pressure and coronary flow on the intracoronary blood volume and geometry of the left-ventricle. Pflugers Archiv. 340:101-111; 1973.
26. Napper, S.A. A mathematical model of oxygen transport in isolated heart. Ph.D. Dissertation, Louisiana Tech University; 1985.
27. Neely, J.R.; Liebermeister, H.; Battersby, E.J.; Morgan, H.E. Effect of pressure development on oxygen consumption by isolated rat heart. Am. J. Physiol. 212(4):804-814; 1967.
28. Neely, J.R.; Whitmer, J.T.; Rovetto, M.J. Effect of coronary blood flow on glycolytic flux and intracellular pH in isolated rat hearts. Circ. Res. 37:733-741; 1975.
29. Nelder, J.A.; Mead, R. A simplex method for functional minimization. Computer J. 7:308; 1965.
30. Olsen, C.O.; Attarian, D.E.; Jones, R.N.; Hill, R.C.; Sink, J.D.; Lee, K.L.; Wechsler, A.S. The coronary pressure-flow determinants of left ventricular compliance in dogs. Circ. Res. 49:856-865; 1981.
31. Opie, L.H. Coronary flow rate and perfusion pressure as determinants of mechanical function and oxidative metabolism of isolated perfused rat heart. J. Physiol. 180:529-541; 1965.
32. Pittman, R.N.; Okusa, M.D. Measurements of oxygen transport in single capillaries. In: Bicher, H.I.; Bruley, D.F., eds. Oxygen transport to tissue—IV. New York: Plenum Press; 1982: pp. 539-553.
33. Rose, C.P.; Goresky, C.A. Interactions between capillary exchange, cellular entry, and metabolic sequestration processes in the heart. In: Renkin, E.; Geiger, S., eds. Handbook of Physiology. Washington, DC: Vol. 4(2), Am. Physiol. Soc.; 1982.
34. Salisbury, P.F.; Cross, C.E.; Rieben, P.A. Influence of coronary artery pressure upon myocardial elasticity. Circ. Res. 8:794-800; 1960.
35. Salisbury, P.F.; Cross, C.E.; Rieben, P.A. Intramyocardial pressure and strength of left ventricular contraction. Circ. Res. 10:608-623; 1962.
36. Scharf, S.M.; Bromberger-Barnea, B. Influence of coronary flow and pressure on cardiac function and coronary vascular volume. Am. J. Physiol. 224(4):918-925; 1973.
37. Schubert, R.W. A physiological and mathematical study of oxygen distribution in the autoregulating isolated heart. Ph.D. Dissertation, Case Western Reserve University; 1976.
38. Schubert, R.W. Myocardial microvascular shunting: Relationship of tissue PO_2 and venous PO_2. Fed. Proc. 37(4):241; 1978.
39. Schubert, R.W.; Fletcher, J.E.; Reneau, D.D. An analytical model for axial diffusion in the Krogh cylinder. In: Bruley, D.F.; Bicher, H.I.; Reneau, D.D., eds. Oxygen transport to tissue—VI. New York: Plenum Press; 1984: pp. 433-442.
40. Schubert, R.W.; Whalen, W.J.; Nair, P. Myocardial PO_2 distribution: Relationship to coronary autoregulation. Am. J. Physiol. 234(4):H361-H370; 1978.
41. Schuchhardt, S.; Losse, B. Static and dynamic behavior of local oxygen pressure in the myocardium. 7th European Conf. Microcirculation, Aberdeen 1972, Part I., Bibl. Anat. No. 11:164-168; 1973.
42. Schwefel, H.P. Numerical optimization of computer models. Great Britain: John Wiley and Sons; 1981.
43. Templeton, G.H.; Wildenthal, K.; Mitchell, J.H. Influence of coronary blood flow on left ventricular contractility and stiffness. Am. J. Physiol. 223(5):1216-1220; 1972.
44. Weisfeldt, M.L.; Shock, N.W. Effect of perfusion pressure on coronary flow and oxygen usage of nonworking heart. Am. J. Physiol. 218(1):95-101; 1970.
45. Whalen, W.J. Intracellular PO_2 in heart and skeletal muscle. Physiologist. 14:69-82; 1971.
46. Wilson, D.F.; Erecinska, M.; Silver, I.A. Metabolic effects of lowering oxygen tension in vivo. In: Bicher, H.I.; Bruley, D.F., eds. Oxygen transport to tissue—IV. New York: Plenum Press; 1982: pp. 293-301.

NOMENCLATURE

C_c = O_2 tension in the capillary [=] mmHg
C_{AO2} = arterial oxygen tension = 722 mmHg
C_{cA} = capillary arterial tension [=] mmHg

C_{cV} = capillary venous tension [=] mmHg
C_t = O_2 tension in the tissue [=] mmHg
D_z^t = axial diffusion coefficient [=] cm^2/min
E = extraction (arteriovenous difference) [=] mmHg
Km = Michaelis-Menten kinetic constant [=] mmHg
L = length of cylinder [=] cm
N = capillary density [=] capillaries/cm^2
P = capillary wall permeability [=] cm/min
PP = perfusion pressure [=] mmHg
Q = whole organ flow rate [=] ml/min-ml(tis)
r_c = radius of capillary [=] cm
r_t = radius of tissue [=] cm
S_o^t = solubility of oxygen [=] moles O_2/ml-min-mmHg
V_{max} = maximum oxygen consumption [=] moles O_2/ml-min
v_z = axial perfusate velocity [=] cm/min
z = axial dimension [=] cm